Surface hydrology in global river basins in the Off-line Land-surface GEOS Assimilation (OLGA) system

Michael G. Bosilovich
Universities Space Research Association, Seabrook, Maryland

Runhua Yang
General Sciences Corporation, Seabrook, Maryland

Paul R. Houser
Hydrologic Sciences Branch / Data Assimilation Office, NASA/GSFC Code 974,
Greenbelt, Maryland

Short title: SURFACE HYDROLOGY IN GLOBAL RIVER BASINS

Abstract.

Land surface hydrology for the Off-line Land-surface GEOS Analysis (OLGA) system and Goddard Earth Observing System (GEOS-1) Data Assimilation System (DAS) has been examined using a river routing model. The GEOS-1 DAS land-surface parameterization is very simple, using an energy balance prediction of surface temperature and prescribed soil water. OLGA uses near-surface atmospheric data from the GEOS-1 DAS to drive a more comprehensive parameterization of the land-surface physics. The two global systems are evaluated using a global river routing model. The river routing model uses climatologic surface runoff from each system to simulate the river discharge from global river basins, which can be compared to climatologic river discharge. Due to the soil hydrology, the OLGA system shows a general improvement in the simulation of river discharge compared to the GEOS-1 DAS. Snowmelt processes included in OLGA also have a positive effect on the annual cycle of river discharge and source runoff. Preliminary tests of a coupled land-atmosphere model indicate improvements to the hydrologic cycle compared to the uncoupled system. The river routing model has provided a useful tool in the evaluation of the GCM hydrologic cycle, and has helped quantify the influence of the more advanced land surface model.

1. Introduction

Data assimilation systems have provided the climate and meteorology community with long-term atmospheric data sets that cover the globe and maintain consistency in time [*Bengsston and Shukla*, 1989; *Daley*, 1991]. The Goddard Earth Observing System (GEOS-1) Data Assimilation System (DAS) produced one of the first long-term reanalyses to use a consistent modeling and assimilation system [*Schubert et al.*, 1993]. In this system, the prescribed land-surface wetness was computed from a bucket model forced with observations of monthly mean precipitation and near-surface atmospheric temperature [see, *Mintz and Serafini*, 1992; *Schemm et al.*, 1992; *Mintz and Walker*, 1993]. While the prescribed soil wetness has some advantages, the resulting GEOS-1 DAS land-surface hydrologic budget was not balanced during the model integration.

Recently, the Off-line Land-surface GEOS Assimilation (OLGA) system has been developed to provide more detailed surface data over the globe. OLGA is a global land surface model driven by near-surface atmospheric data from the GEOS DAS reanalysis. The *Koster and Suarez* [1992, 1996] Mosaic land-surface model provides the core of the surface physical parameterizations including surface heat and water budgets.

The present study evaluates the influence of OLGA's active land surface calculations compared to the GEOS-1 prescribed soil wetness on the modeling of global climate land-surface hydrology. An important and sensitive component of surface hydrology is the runoff water. Here, we define the source runoff water as the runoff water that is produced from the model hydrology at the GCM grid. While runoff water observations are generally not available, the discharge of water at river mouths is routinely observed. Note the distinction between source runoff water and river discharge.

In order to close the general circulation model (GCM) hydrology, the river routing model developed by *Miller et al.* [1994] routes GCM source runoff water through a river system to simulate the river discharge of numerous basins around the Earth. The comparison of model and observed river discharge is a rigorous validation of the surface

model's ability to simulate important physical processes such as snowmelt.

In the OLGA and GEOS-1 simulations, interaction between the surface soil water and precipitation does not occur. While OLGA soil water is predicted based on precipitation, it does not change the precipitation. Soil water can influence precipitation processes in a variety of ways [*Mintz*, 1984; *Beljaars et al.*, 1996; *Bosilovich and Sun*, 1998], and ultimately, the interactions must be included in numerical simulations. The next generation of the GEOS-DAS will incorporate the Mosaic LSM as its surface boundary. The interactive surface model has already been successfully implemented into the GEOS-GCM. We will also present hydrology results from the coupled GEOS-GCM and LSM.

2. Methodology

In this section, we summarize OLGA and GEOS-1 DAS specifically focusing on the surface hydrology modeling strategies. The river routing model and the observations of precipitation and river discharge are also described.

2.1. Off-line Land-surface GEOS Assimilation (OLGA) System

The Off-line Land surface GEOS Assimilation (OLGA) system [*Houser et al.*, 1998] is being developed as a testbed for developing land data assimilation strategies for the fully coupled GEOS-DAS. Therefore, to the greatest extent that is reasonable, the OLGA system has been designed to mimic the fully-coupled system, with the vision of eventually implementing techniques developed off-line into the full GEOS-DAS. The OLGA system is proving to be an excellent resource for efficiently testing new land surface data assimilation strategies, and allows for the off-line replacement of often biased GCM land surface forcing fields (such as precipitation and radiation) with observed quantities.

The OLGA system was implemented globally over land at a $2° \times 2.5°$ resolution for

the 14 years of available GEOS-1 DAS reanalysis forcing (1981 through 1995). The 3 hour GEOS-1 DAS forcing data was linearly interpolated in time to the 5 minute OLGA time step. The International Satellite Land-Surface Climatology Project (ISLSCP) initiative 1 land cover definitions specify vegetation in OLGA [*Meeson et al.*, 1995; *Sellers et al.*, 1995]. A five year OLGA simulation was used to spin-up the inital state for the present simulation. The OLGA surface data sets are currently being offered as a supplement to the inactive land surface present in the GEOS-1 DAS.

Mosaic [*Koster and Suarez*, 1992, 1996] is the current Land Surface Model (LSM) implemented in OLGA. The Mosaic model is based on sound, well- accepted theory that has been proven by: (1) its superior performance in several model intercomparison studies including the Project for the Intercomparison of Land Surface Schemes (PILPS) [*Henderson-Sellers et al.*, 1993]; (2) its ability to produce stable land surface conditions and realistic climate simulations in the NASA/GSFC Aries GCM [*Suarez et al*, 1996; and (3) the high correlation between Mosaic predictions and in-situ observations of surface fluxes and states made during several intensive field campaigns.

The Mosaic LSM was originally derived from the Simple Biosphere (SiB) model developed by *Sellers et al.* [1986]. Mosaic, however, accounts for sub-grid scale heterogeneity by dividing each GCM grid into homogeneous sub-regions. Furthermore, each sub-region is associated with a shallow profile of model atmospheric grid points. This permits partial surface atmosphere interactions, but only near the surface, not with the large-scale environment.

The data that drive OLGA are the atmospheric state (temperature, moisture and wind), the downwelling shortwave and longwave radiation, surface pressure and precipitation. Mosaic maintains eight prognostic variables, which include the surface skin and deep soil temperatures, the canopy vapor pressure, and the moisture content of the snowpack, interception reservoir and soil layers. A percentage of the incoming radiative energy to the land surface is reflected, and the remainder that is absorbed

is partitioned into upwelling longwave radiation, snowmelt, and sensible, latent, and ground heat fluxes. The partitioning of energy fluxes is controlled by a series of resistances that vary with environmental stress, and heat flow into the soil is performed using a force-restore method. Precipitation falling on the land surface is partitioned into canopy interception, surface runoff, or infiltration into the first of three soil layers. Water diffuses between these three layers, and can percolate out of the third layer. Water can be evaporated from the interception reservoir and the snowpack, and can be extracted by plants from the top two soil layers for transpiration. *Koster and Suarez* [1996] discuss the water and energy conservation calculations in greater detail. For the present work, the calculation of runoff water is described below.

The rate of total source runoff, R, is generated in Mosaic as the sum of the surface runoff rate, R_s, and the baseflow or moisture diffusion flux out of the bottom of the lowest soil layer, $Q_{3\infty}$:

$$R = R_s + Q_{3\infty} \tag{1}$$

The surface runoff rate, R_s, is equal to the rate of rain throughfall, P_T, less infiltration:

$$R_s = P_T - \frac{W_1 - [W_1]_{old}}{\Delta t} \tag{2}$$

where W_1 is the moisture in the top layer, Δt is the time step length, and the subscript *old* denotes quantities calculated at the previous time step. The moisture in the top layer is updated by adding the smaller of either the throughfall onto dry soil, P_{T-dry}, or the unused top layer moisture capacity, W_{1-add}:

$$W_1 = [W_1]_{old} + \min(P_{T-dry}, W_{1-add}) \tag{3}$$

Mosaic soil hydrology calculations are divided into two sub-areas, one that is fully saturated and the other whose degree of saturation is W_{1-eq}/W_{1-sat}. W_{1-eq} is the water content in the top soil layer that would be in equilibrium (according to Richards equation) with the water content in the middle soil layer, and W_{1-sat} is the moisture

holding capacity of the top soil layer. Given that W_1 is the total amount of water in the top soil layer, the saturated fraction, f_{sat}, can be computed as:

$$f_{sat} = \begin{cases} \frac{W_1 - W_{1-eq}}{W_{1-sat} - W_{1-eq}} & W_1 > W_{1-eq} \\ 0 & W_1 < W_{1-eq} \end{cases} \tag{4}$$

Then, the throughfall mass falling on the dry fraction is:

$$P_{T-dry} = P_T(1 - f_{sat})\Delta t \tag{5}$$

and the unused moisture capacity of the top layer is:

$$W_{1-add} = f(W_{1-sat} - W_{1-eq})(1 - f_{sat}) \tag{6}$$

where f is the fractional coverage of precipitation.

Percolation out of the bottom of the lowest soil layer, $Q_{3\infty}$, is computed with a bulk form of Richards equation in which only gravitational drainage operates, and the presence of bedrock is allowed to reduce the flow:

$$Q_{3\infty} = \rho_\omega K_3 \sin(\theta) \tag{7}$$

where θ is the bedrock angle, K_3 is the hydraulic conductivity of the lowest soil layer, and ρ_ω is the density of liquid water.

2.2. Goddard Earth Observing System (GEOS)

The GEOS-1 DAS has produced a multi-year global atmospheric data set for use in climate and weather studies [*Schubert et al.*, 1993]. The GEOS-1 GCM is described by *Takacs et al.* [1994] and *Molod et al.* [1996]. *Pfaendtner et al.* [1995] document the DAS. *Bosilovich and Schubert* [1998] discuss the GEOS-1 DAS surface parameterization in detail.

A simple bucket model specifies the GEOS-1 DAS monthly mean soil wetness off-line. The bucket model uses observed monthly mean precipitation and temperature

as input [*Schemm et al.*, 1992], similar to the procedure of *Mintz and Serafini* [1992]. The prescribed soil wetness should provide lower boundary forcing that resembles observations and cannot drift toward unrealistic values. While modeled precipitation may be biased, the bias will not feed back into the atmospheric system through the soil wetness. However, without an interactive hydrologic balance at the surface, the long term integration of evaporation no longer depends on the modeled precipitation. Runoff water is diagnosed from monthly mean soil water, precipitation and evaporation after the completion of the model integration.

For each month during the period from January 1985 through December 1993, monthly mean runoff is computed by,

$$R_o = P - E - \frac{\partial W}{\partial t}. \tag{8}$$

Here, P and E are the monthly mean precipitation and evaporation, respectively. R_o is the source runoff. While the monthly mean storage of water ($\partial W/\partial t$) is generally small, it cannot be neglected in the annual cycle. Because the storage of water is prescribed prior to the integration of the GEOS-1 reanalysis, this diagnostic computation can yield $R_o < 0$. Uncertainty of the evaporation based on the prescribed soil wetness and the inability of the storage of water to react to $P - E$ lead to negative values of runoff, which is unrealistic in the climate system [See also, *Arpe*, 1998]. If at a grid point $R_o < 0$, then that month's value of runoff is set to zero, and the negative value is integrated into a residual variable. The residual variable is saved to indicate the amount of imbalance in the GEOS surface hydrology. Hence, only positive values of runoff from Eq. 8 are included in the computation of GEOS-1 climate annual cycle of runoff.

Presently, the Mosaic land surface model (LSM) [*Koster and Suarez*, 1992, 1996] is being incorporated into the GEOS DAS. The LSM is identical to that applied in OLGA. Hence, future versions of the GEOS system will not be limited by the same deficiencies noted in this section. Some preliminary results of the GEOS GCM coupled with Mosaic

LSM will also be presented.

2.3. River Routing Model

The river routing model was developed to provide closure to GCM hydrology budgets and to allow validation of GCM source runoff [*Miller et al.*, 1994]. Climate mean source runoff of GCMs (R_o) provides the forcing for the river routing (again, noting the difference between source runoff and river discharge defined earlier). In order to move the water from grid spaces to the river mouth, the routing model requires an algorithm for the river mass flow and a river direction file based on the topographic gradient. *Miller et al.* [1994] provide a complete list and map of all the river basins. Forty-seven river basins are defined in the river routing model with $2° \times 2.5°$ resolution.

The flux of water from a grid box (F in kg s^{-1}) is given by,

$$F = M \times \frac{u}{d}. \tag{9}$$

Where, M is the river mass above the sill depth, d is the mean distance between the grid box and its downstream neighbor, and u is an effective flow rate of water from a grid box to its downstream neighbor, depending on the downstream topography gradient. During a time step, the change in river mass in a grid box is given by,

$$M(t + \Delta t) - M(t) = R_o + \Delta t \Sigma F_{IN} - \Delta t F_{OUT}. \tag{10}$$

Where, F_{OUT} is the flux of water that leaves a grid box, and ΣF_{IN} is the flux of water entering a grid box. Eventually, the water is moved to the river mouth, where it is defined as the river discharge.

The resulting river discharge comparison with observations identifies strengths and weaknesses in the GCM hydrology, but it must be carefully examined. The river routing model cannot ameliorate the effect of errors in GCM evaporation and precipitation on the river discharge. In addition, several river flow parameters are specified globally, for

lack of detailed observations. Some processes are not explicitly included in the river routing model, such as freezing rivers (though the Mosaic LSM does freeze soil water) and ice flow.

2.4. Observations

We use two types of observed data for verification: river discharge from over thirty-seven river basins and gridded precipitation. The monthly mean river discharge data were provided by Global Runoff Data Center, Federal Institute of Hydrology, Germany. The climatological monthly mean river discharge were computed for the period of January 1979 to December 1988. The observed monthly mean precipitation were merged Microwave Sounding Unit version-1 over oceans blended with rain gauge data over land at $4° \times 5°$ resolution. The climatological monthly mean values were computed for the same 10 years as the river discharge data [*Lau et al.*, 1996]. These precipitation data over land were also used to compute the GEOS-1 soil wetness boundary condition [*Schemm et al.*, 1992].

For comparison purposes, we approximate the basinwide observed evaporation using the climate mean river discharge and basin averaged precipitation observations. It is assumed that in a climate mean average the river discharge approximates area averaged grid space runoff, and that the climate change of soil water is negligible. Therefore, by averaging equation 8 for the annual cycle, the climate mean basinwide evaporation can be computed by

$$E = P - R_d. \tag{11}$$

All the uncertainty in both precipitation and river discharge (R_d) will then be reflected in E.

3. Results

3.1. Basinwide Climate Hydrology

We approximate the annual mean basinwide observed evaporation assuming that it is equal to the difference of annual mean precipitation and river discharge. Figure 1 shows the climate mean evaporation and evaporative fraction (E/P) for 25 of the modeled river basins (sorted by decreasing observed river discharge). In most of the basins, and especially the largest, GEOS-1 tends to over estimate the evaporation. While OLGA's evaporation tends to be less than (or equal to) that of GEOS-1, it is still larger than the observed residual evaporation in many basins. This may be related to GEOS-1 small overestimate of precipitation in many of the river basins.

Figure 1

The lack of surface hydrology balance in GEOS-1 is apparent in the basinwide climate mean evaporative fraction (Figure 1b). In many basins, GEOS-1 evaporative fraction is unrealistic for a climate mean (E/P $>$ 1). OLGA's evaporative fraction tends to be closer to observations and it is always less than one for a basinwide climate average. The reason for this drop in evaporation is because OLGA conserves water in the soil, and in GEOS-1, the soil water does not interact with the evaporation.

Figure 2 shows the observed annual mean river discharge observations (area averaged) and model basinwide average grid point runoff. There are a few river basins where OLGA and GEOS clearly have difficulty to simulate the hydrology. However, there are more basins where the differences from observations are not very large. Because the GEOS-1 DAS runoff was diagnosed by using a hydrologic balance (neglecting the negative values of runoff), the annual mean of the GEOS-1 runoff is similar to that of OLGA. As we will show in the next section, the major differences between the two cases are in the representation of the annual cycle.

Figure 2

3.2. OLGA and GEOS-1 DAS Annual Cycles

While there may be many sources of uncertainty in the simulated river discharge (as discussed previously), much may still be learned about the model's hydrology. For example, Amazon river discharge is particularly difficult to simulate. *Lau et al.* [1996] find that many GCM's cannot generate as much river discharge as observed. Also, using the river routing model, coupled with the Goddard Institute for Space Studies GCM, *Miller et al.* [1994] strongly underestimate the Amazon's river discharge. In the present study, the Amazon precipitation is very large but comparable to observation (Figure 3). Figure 3
The source runoff for both OLGA and GEOS-1 are very similar, with OLGA slightly lagging behind GEOS-1. Overall, there are only small differences between the two models' river discharge.

In the Congo river basin, GEOS-1 tends to overestimate precipitation, leading to the overestimate of river discharge in both OLGA and GEOS-1 (Figure 4). However, Figure 4
the phase of OLGA river discharge has improved compared to GEOS-1. While the more detailed land-surface processes in OLGA help improve the river discharge in the Congo, this is not always the case (as in the Amazon).

As discussed by *Boyle* [1998], GCMs tend to over estimate spring and summer rainfall amounts in the United States. This has been known for some time in the GEOS-1 DAS [*Schubert et al.*, 1995], and it is quite apparent in these results (Figure 5). Figure 5
In the Mississippi river basin, the high summer precipitation dominates the simulate river discharge. *Beljaars et al.* [1996] results suggest that better representation of the surface water content can improve the simulation of precipitation. The poor summer precipitation in GEOS-1 could be related to the simplistic surface representation.

The northern river basins in OLGA exhibit substantial improvement of both source runoff and river discharge. The Volga river basin is a good example (Figure 6), but Figure 6
this result is also true for other basins (Amur, Ob and somewhat noticeable in the Mississippi). The snowmelt clearly affects the river discharge simulation, but there are

still differences between OLGA and observations. This could be the result of either less winter precipitation (snow) or an underestimate of the river flow rates in the river routing model. The GEOS-1 system, however, does not include snowmelt processes. The influence of the Mosaic LSM snowmelt in OLGA is quite apparent in the source runoff, especially compared to GEOS-1 (March and April source runoff in Figure 6b).

3.3. GEOS GCM with Interactive Land Surface Processes

In the previous discussion, the coupled land-surface interactions are not included in either the OLGA or GEOS-1 systems. The interaction between surface and atmosphere will influence the precipitation, evaporation and the river discharge (among other processes). An ongoing effort to incorporate the Mosaic LSM into the GEOS GCM has produced some preliminary results. Here, we present results from the GCM coupled with the Mosaic LSM (GCM-LSM) and GCM with the same surface parameterization as in GEOS-1 (Control). The GCM resolution is $4° \times 5°$, and both GCM cases were integrated for 5 years. Note that the GEOS-1 DAS reanalyses includes observational data assimilated into the GCM global system. In this experiment, the GCM simulations do not include the assimilated observations.

The influence of the coupled system on the Mississippi river basin precipitation is quite clear (Figure 7). In the Control simulation, the precipitation is very large in spring and summer, much like that of GEOS-1, leading to a substantial overestimate of the river discharge. With the coupled LSM, the spring and summer precipitation is much less than control and closer to observations. However, autumn precipitation, which is a valuable recharge source in the annual hydrologic cycle, is underestimated. This leads to low springtime river discharge. For the climate mean over the entire annual period, the both precipitation and river discharge are much closer to observed than the Control.

Figure 7

The GCM-LSM simulation of snowmelt processes is much better than the Control simulation. The Control Volga river basin exhibits large river discharge in the winter

due to the lack of simulated snow processes. The GCM-LSM, however, includes snow processes, and produces a strong snowmelt signature in the model source runoff during late spring (Figure 8). The resulting simulated river discharge shows a similar pattern to the observations, but lags two months behind. There is some indication that, for this simulation, the early spring temperatures were too cold to permit snowmelt (maintaining the snowcover till late spring). In addition, this may indicate that the globally defined flow rate variables may not be well suited for this basin or particular simulation [*Miller et al.*, 1995]. Optimizing the flow rates within the river routing model for use with the GEOS systems is beyond the scope of this study. However, the next section presents some possibilities for future improvements to the river routing.

Figure 8

3.4. Error analysis and sensitivity

The river flow rate (in eq. 9) is computed as a function of the topographic gradient. In the vicinity of the river mouth, topographic gradients tend to be small. To prevent the flow rate from becoming too small, a minimum flow rate is imposed for all river basins. *Miller et al.* [1994] find that the river discharge is sensitive to this value. Because it appears that there may be lag in some of the simulated river discharge, we examine the influence of the minimum flow rate on river discharge error.

River discharge errors for each simulation were computed for the river basins and global average following *Miller et al.* [1994] (their equations 10 and 12 respectively). The observed river discharge normalizes the error so that a value of zero indicates complete correspondence between model and observation. *Miller et al.* [1994] found a value of 0.566 global river discharge error in their simulations. These errors represent a combination of errors in precipitation and evaporation, as well as the river routing. However, the normalized global runoff error is weighted by normalized monthly mean precipitation error.

In the present models, global error from the Mosaic LSM (either OLGA or

GCM-LSM simulation) is generally smaller compared to their control counterparts (Figure 9 a). For each set of experiments, the simulation that includes the LSM tends to reduce the minimum error by about 0.05. The GCM Control simulation shows significant sensitivity to the minimum flow rate, while the GCM-LSM simulations is essentially insensitive. The OLGA river discharge improves for increasing minimum flow rate (up to 0.30 ms^{-1}), while the GEOS-1 system's lowest error occurs for smaller minimum flow rates (0.15 ms^{-1}). This indicates that a process in OLGA is slowing down the movement of water from precipitation to the river discharge compared to GEOS-1. One possible mechanism is the vertical diffusion of water in the LSM.

Figure 9

The river discharge error for several river basins in the OLGA simulation is examined more closely (Figure 9 b). Four of the selected river basins (Amur, Ob, Amazon and Yangtze) reflect the OLGA global error, with minimum error values occurring at 0.30 ms^{-1}. The Ob and Amur river discharge error decreases rapidly for small changes of low flow rate. The Volga river error continues to decrease for fairly high values of the speed (0.80 - 1.0 ms^{-1}). This is related to increasing the speed at which the snowmelt water reaches the river mouth (see also Figure 6).

The difficulty in choosing a representative minimum flow rate is apparent in the error for the Mississippi and Congo basins. The Mississippi error starts at a high value and the error decreases with higher speeds, while the Congo starts at its lowest value and increases with increasing speed. We have not attempted to optimize the river routing simulations presented here because each GCM and the river basins require improved values that describe the river flow.

4. Summary and Conclusions

OLGA and GEOS-1 DAS land surface hydrology has been examined using a river routing model. The GEOS-1 DAS land-surface parameterization is fairly simple, including an energy balance and prescribed soil water. OLGA uses near-

surface atmospheric data from the GEOS-1 DAS to drive a more comprehensive parameterization of the land-surface physics. The two global systems are evaluated using a global river routing model [*Miller et al.*, 1994]. The river routing model uses climatologic surface runoff from each system to simulate the river discharge from several river basins. The results are compared with river discharge observations.

In general, the more detailed physical processes incorporated into the OLGA system produce more reasonable river discharge than the GEOS-1 DAS. This is most likely related to the influence of prescribed soil water on GEOS-1 DAS evaporation an precipitation. Snowmelt processes included in OLGA have a positive effect on the annual cycle of river discharge and source runoff. Improved river flow characteristics could help reduce errors in the simulated river discharge. The river routing model, however, was not optimized because simulation is sensitive to both the GCM and the individual river basin.

Simulations with a coupled GCM-LSM indicated that the LSM has a substantial effect on the entire hydrologic cycle in the GEOS GCM. In general, the LSM provided improvements to the hydrology. The snow melt, again, appears to be improved over the GEOS-1 system. However, the phase of the discharge was two months too late. Also, the Mississippi River basin precipitation was only partially improved in the coupled system. These are preliminary results, and the effort will continue with longer GCM simulations and data assimilations. The river routing model has provided a useful tool in the evaluation of the GCM hydrologic cycle, and has helped quantify the influence of the more advanced land surface model.

Acknowledgements. We would like to express our thanks to J. H. Kim for providing the merged precipitation data, Dr. Grabs at GRDC for the river discharge data and Dr. G. L. Russell for providing the river routing model and data files. This work was partially supported by NASA contract NAS5-32484.

References

Arpe, K., Comparison of fresh water fluxes in the ECMWF, NCEP and GEOS-1 reanalyses, Proceedings of the First WCRP International Conference on Reanalyses, WMO/TD-NO.876, WCRP-104, 97 - 100, 1998.

Beljaars, A.C.M., P. Viterbo, M. Miller, and A. Betts, The anomalous rainfall over the United States during July 1993: Sensitivity to land surface parameterization and soil moisture anomalies, *Mon. Wea. Rev., 124*, 362 - 383, 1996.

Bengtsson, L. and J. Shukla, Integration of space and in situ observations to study global climate change, *Bull. Am. Meteor. Soc., 40*, 1130-1143, 1989.

Bosilovich M. G., and S. D. Schubert, A comparison of GEOS assimilated data with FIFE observations, *NASA Technical Memorandum No. 104606, vol.* , Goddard Space Flight Center, Greenbelt, MD, 1998.

Bosilovich, M. G., and W.-Y. Sun, Numerical simulation of the 1993 Midwestern flood: Land-atmosphere interactions, *J. Climate*, , IN PRESS, 1998.

Boyle, J. S., Evaluation of the annual cycle of precipitation over the United States in GCMs: AMIP Simulations, *J. Climate, 11*, 1041 - 1055, 1998.

Daley, R., *Atmospheric Data Analysis*, Cambridge University Press, 1991.

Henderson-Sellers, A., Z. -L. Yang, and R. E. Dickinson, The project for the intercomparison of land surface parameterization schemes (PILPS), *Bull. Am. Meteor. Soc., 74*, 1335-1349, 1993.

Houser, P., R. Yang, J. Joiner, A. Da Silva, and S. Cohn, Land Surface GEOS assimilation strategy, Data Assimilation Office Note, Goddard Space Flight Center, Greenbelt, MD 20771.

Koster, R. D., and M. J. Suarez, Modeling the land surface boundary in climate models as a composite of independent vegetation stands, *J. Geophys. Res, 97*, 2697 - 2715, 1992.

Koster, R. D., and M. J. Suarez, Energy and water balance calculations in the Mosaic

LSM, *NASA Technical Memorandum No. 104606, vol. 9*, Goddard Space Flight Center, Greenbelt, MD, 1996.

Lau, K.-M., J. H. Kim and Y. Sud, Intercomparison of hydrologic processes in AMIP GCMs, *Bull. Am. Meteor. Soc., 77*, 2209 - 2227, 1996.

Meeson, B. W., F. E. Corprew, J. M. O. McManus, D. M. Myers, J. W. Clos, K. -J. Sun, D. J. Sunday, P. J. Sellers, 1995. ISLSCP Initiative I-Global Data Sets for Land-Atmosphere Models, 1987-1988. Volumes 1-5. Published on CD by NASA.

Miller, J. R., G. L. Russell and G. Caliri, Continental-scale river flow in climate models, *J. Climate, 7*, 914 - 928, 1994.

Mintz, Y., *Global Climate*, Cambridge, 233 pp., 1984.

Mintz, Y. and Y. V. Serafini, A global monthly climatology of soil-moisture and water-balance, *Clim. Dynam., 8*, 13 - 27, 1992.

Mintz, Y. and G. K. Walker, Global Fields of soil moisture and land surface evapotranspiration derived from observed precipitation and surface air temperature, *J. Appl. Meteorol., 32*, 1305 - 1334, 1993.

Molod, A., H. M. Helfand and L. Takacs, The climatology of parameterized physical processes in the GEOS-1 GCM and their impact on the the GEOS-1 Data Assimilation System, *J. Climate, 9*, 764 - 785, 1996.

Pfaendtner, J., S. Bloom, D. Lamich, M. Seablom, M. Sienkiewicz, J. Stobie, and A. da Silva, Documentation of the Goddard Earth Observing System Data Assimilation System - Version 1, *NASA Technical Memorandum No. 104606, vol. 4*, Goddard Space Flight Center, Greenbelt, MD, 1995.

Schemm, J., S. D. Schubert, J. Terry and S. Bloom, Estimates of monthly mean soil moisture for 1979-1989, *NASA Technical Memorandum No. 104571*, Goddard Space Flight Center, Greenbelt, MD, 1992.

Schubert, S. D., J. Pfaendtner and R. Rood, An assimilated data set for Earth science applications, *Bull. Am. Meteor. Soc., 74*, 2331 - 2342, 1993.

Schubert, S. D., C.-K. Park, C.-Y. Wu, W. Higgins, Y. Kondratyeva, A. Molod, L. Takacs, M. Seablom, and R. Rood, A multiyear assimilation with the GEOS-1 System: Overview and results, *NASA Technical Memorandum No. 104606, vol. 6*, Goddard Space Flight Center, Greenbelt, MD, 1995.

Sellers, P. J., B. W. Meeson, J. Closs, J. Collatz, F. Corprew, D. Dazlich, F. G. Hall, Y. Kerr, R. Koster, S. Los, K. Mitchell, J. McManus, D. Myers, K. -J. Sun, P. Try, An Overview of the ISLSCP Initiative I Global Data Sets: ISLSCP Initiative I - Global Data Sets for Land- Atmosphere Models 1987-1988, Volumes 1-5, Published on CD by NASA, 1995.

Sellers, P. J., Y. Mintz, and A. Dalcher, A simple biosphere model (SiB) for use within general circulation models, *J. Atmos. Sci.*, *43*, 505-531, 1986.

Suarez, M. J., and L. L. Takacs, Documentation of the Aries/GOES Dynamical Core Version 2, *NASA Technical Memorandum No. 104606, vol. 5*, Goddard Space Flight Center, Greenbelt, MD, 1996.

Takacs, L. L., A. Molod and T. Wang, Documentation of the Goddard Earth Observing System General Circulation Model - Version 1, *NASA Technical Memorandum No. 104606, v. 1*, Goddard Space Flight Center, Greenbelt, MD, 1994.

Michael G. Bosilovich, Universities Space Research Association, NASA/GSFC Code 910.3, Greenbelt, MD 20771, email: mikeb@dao.sfc.nasa.gov

Runhua Yang, General Sciences Corporation, NASA/GSFC Code 910.3, Greenbelt, MD 20771

Paul R. Houser, Hydrological Sciences Branch and Data Assimilation Office, NASA/GSFC Code 974, Greenbelt, MD 20771

Received _____

List of Figures

5. Figures

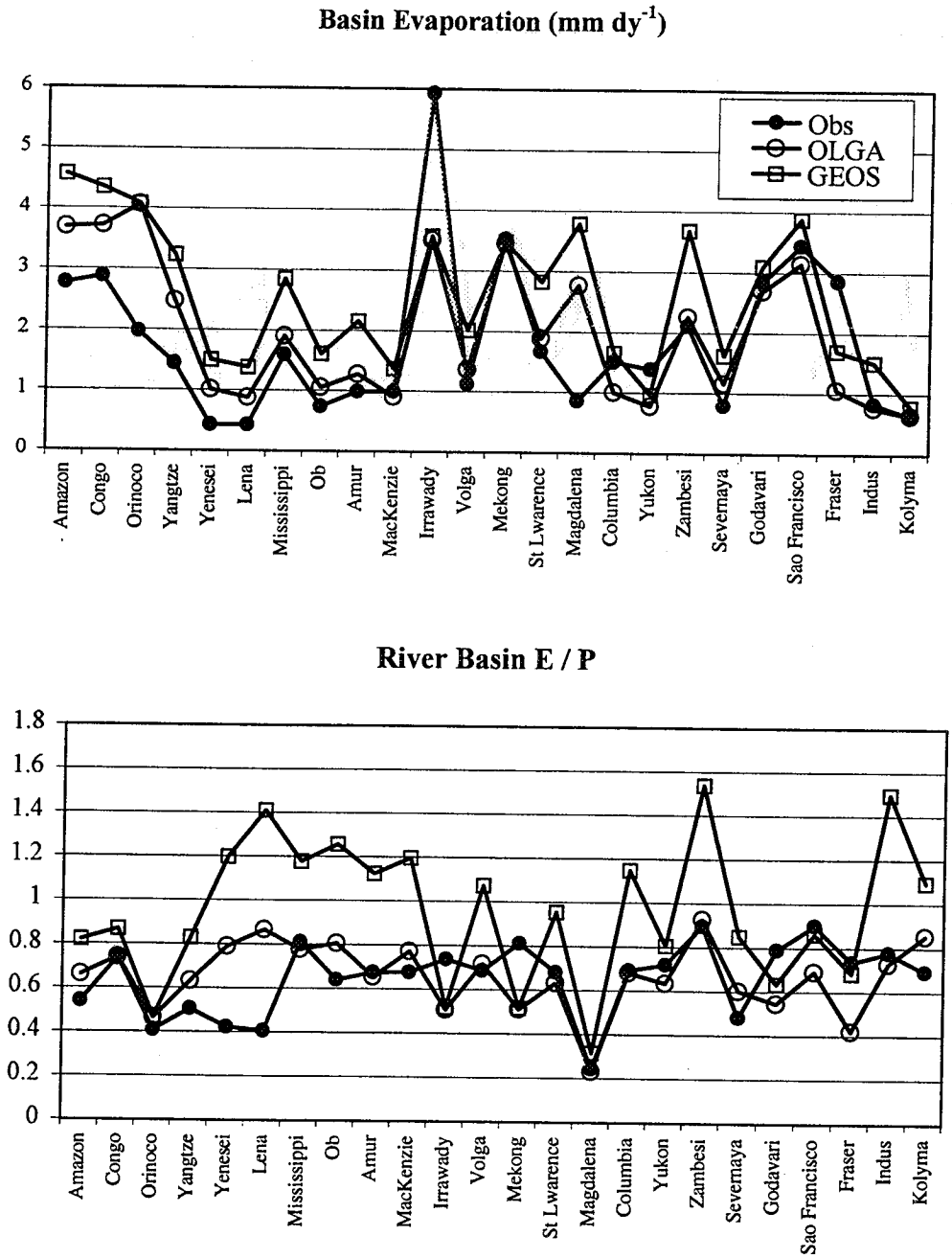

Figure 1. Annual mean evaporation ($mm\ dy^{-1}$) and evaporative fraction (E/P).

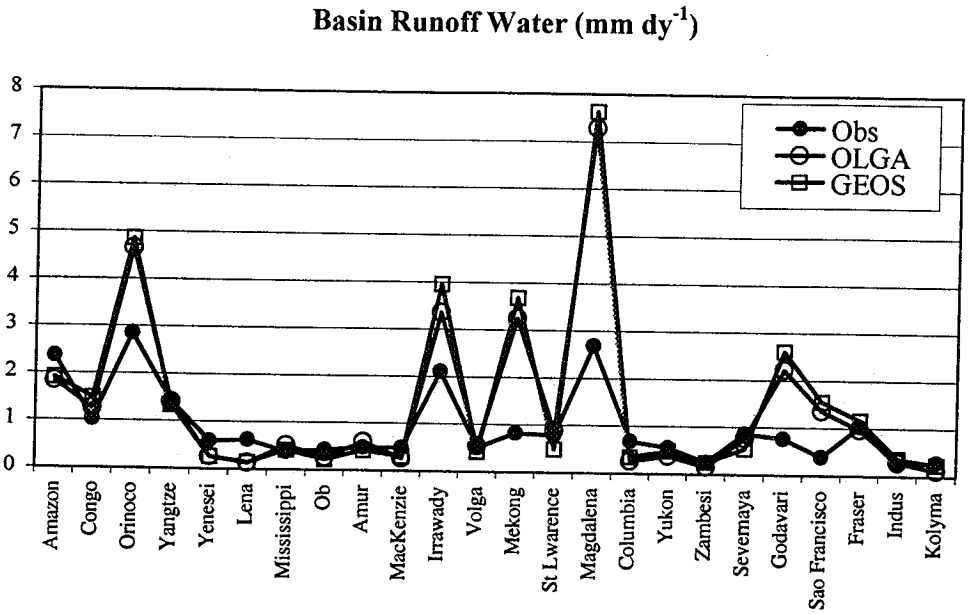

Figure 2. Annual mean basin average runoff water ($mm\ dy^{-1}$).

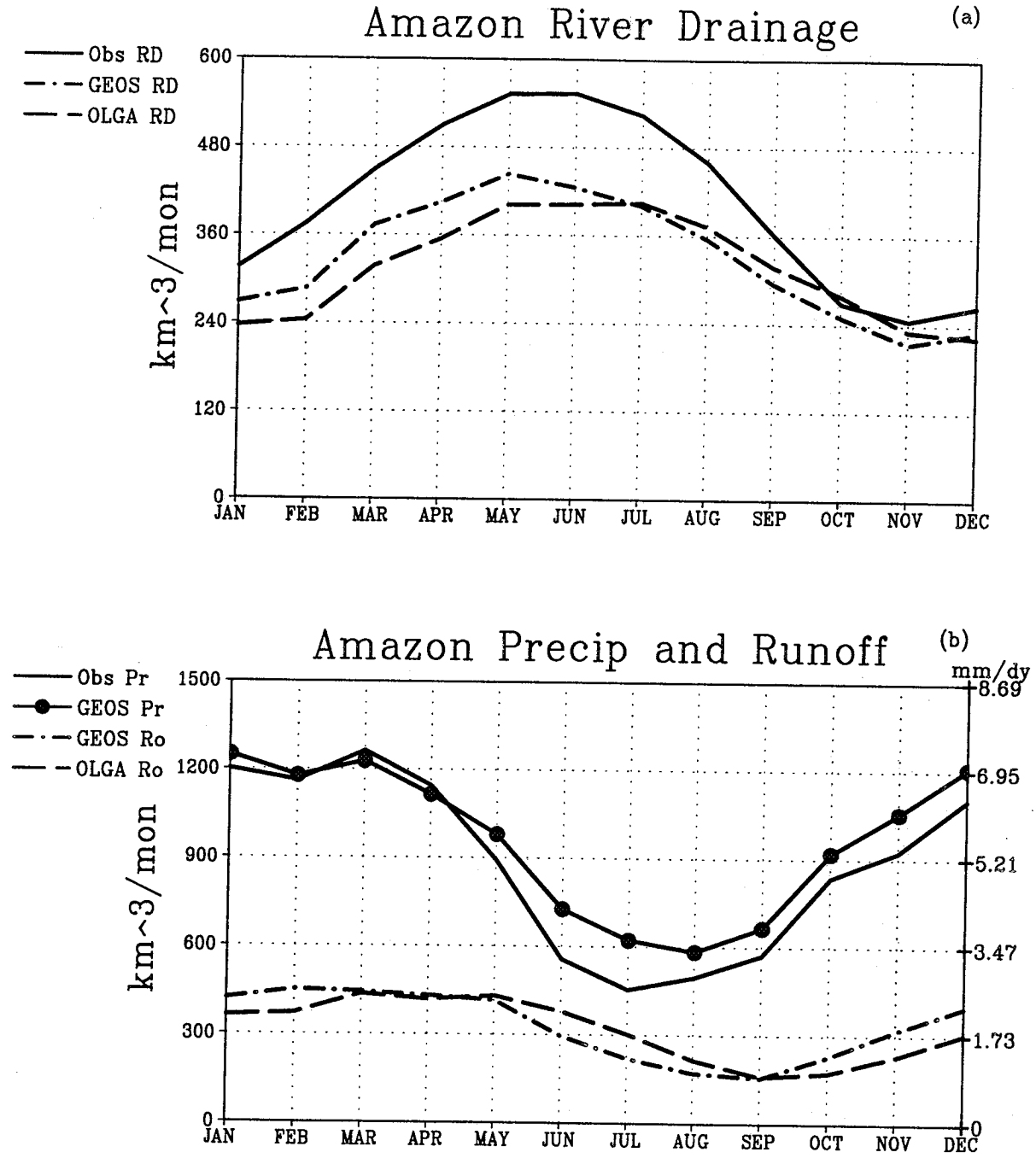

Figure 3. Annual cycle of (a) river discharge from the Amazon River basin for observations, OLGA and GEOS-1 DAS, and (b) precipitation and model source runoff.

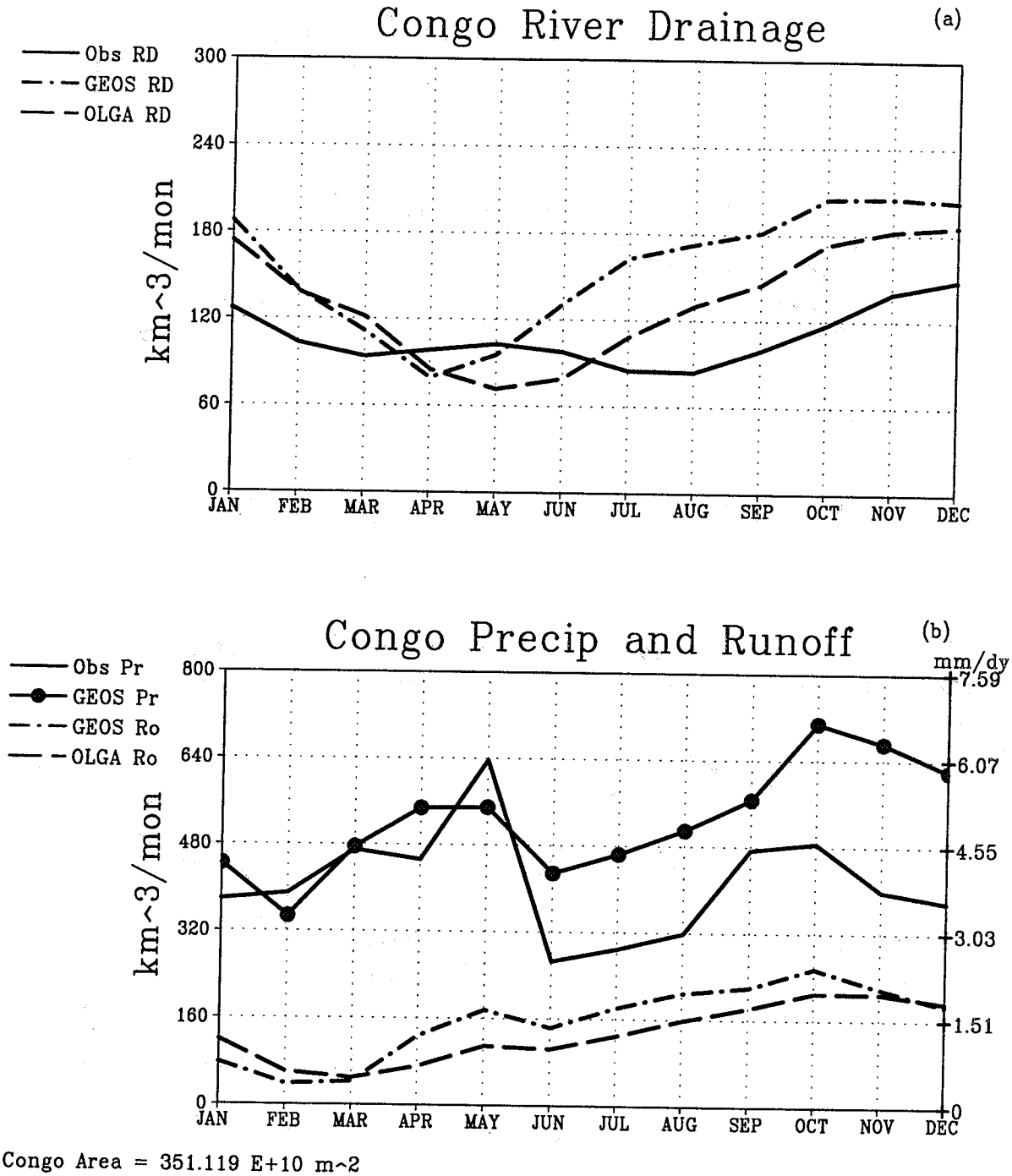

Figure 4. Annual cycle of (a) river discharge from the Congo River basin for observations, OLGA and GEOS-1 DAS, and (b) precipitation and model source runoff.

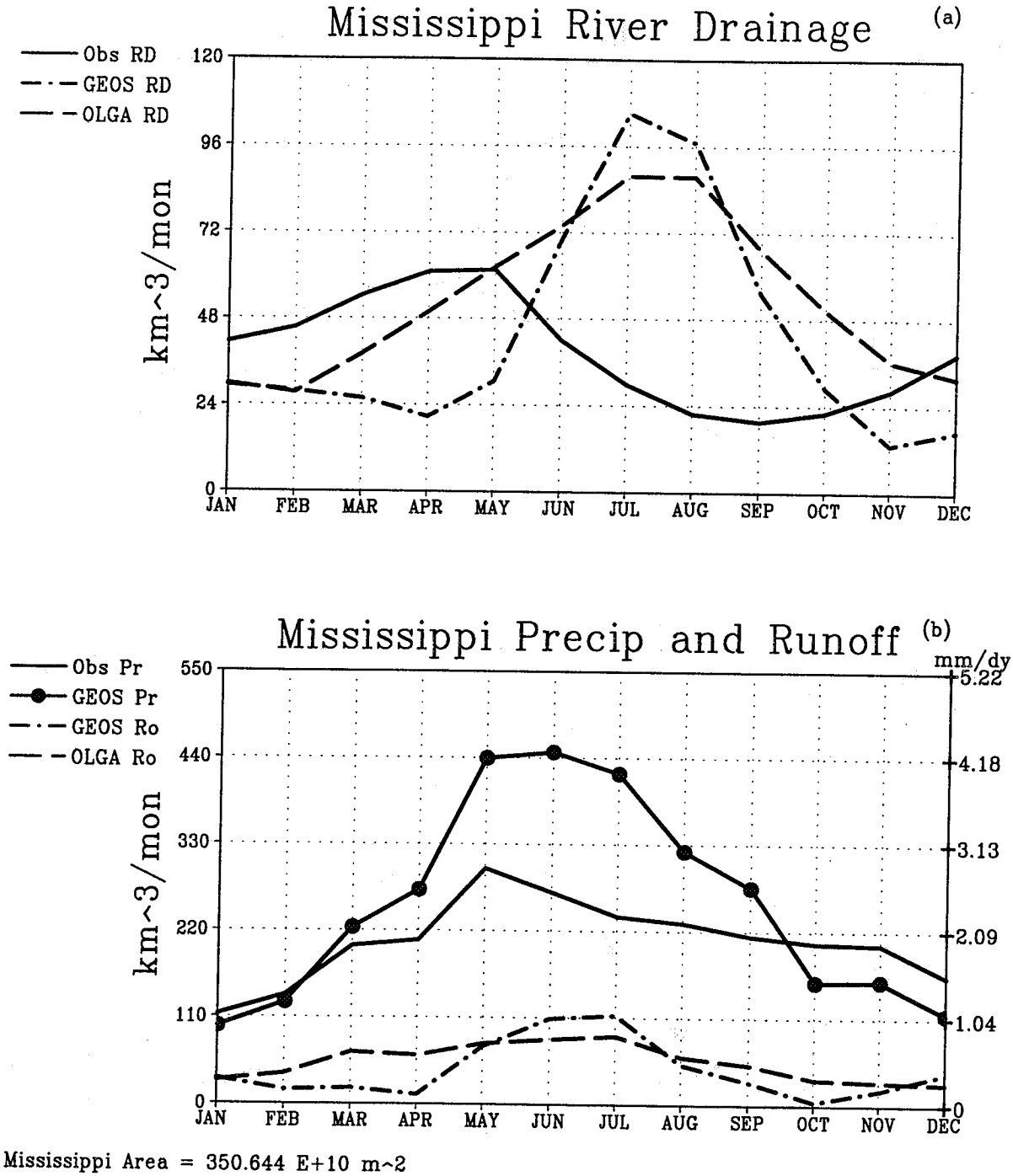

Figure 5. Annual cycle of (a) river discharge from the Mississippi River basin for observations, OLGA and GEOS-1 DAS, and (b) precipitation and model source runoff.

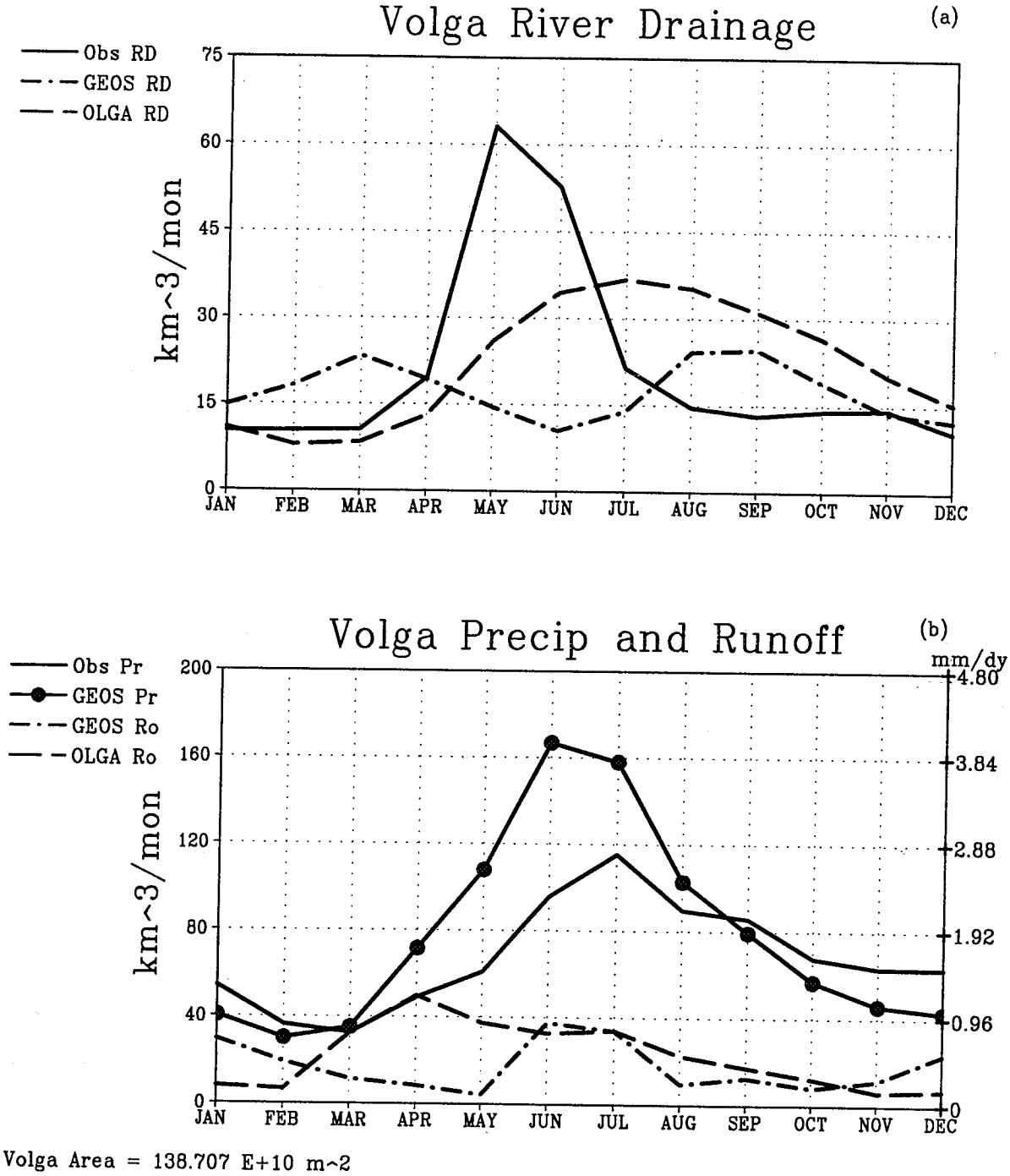

Figure 6. Annual cycle of (a) river discharge from the Volga River basin for observations, OLGA and GEOS-1 DAS, and (b) precipitation and model source runoff.

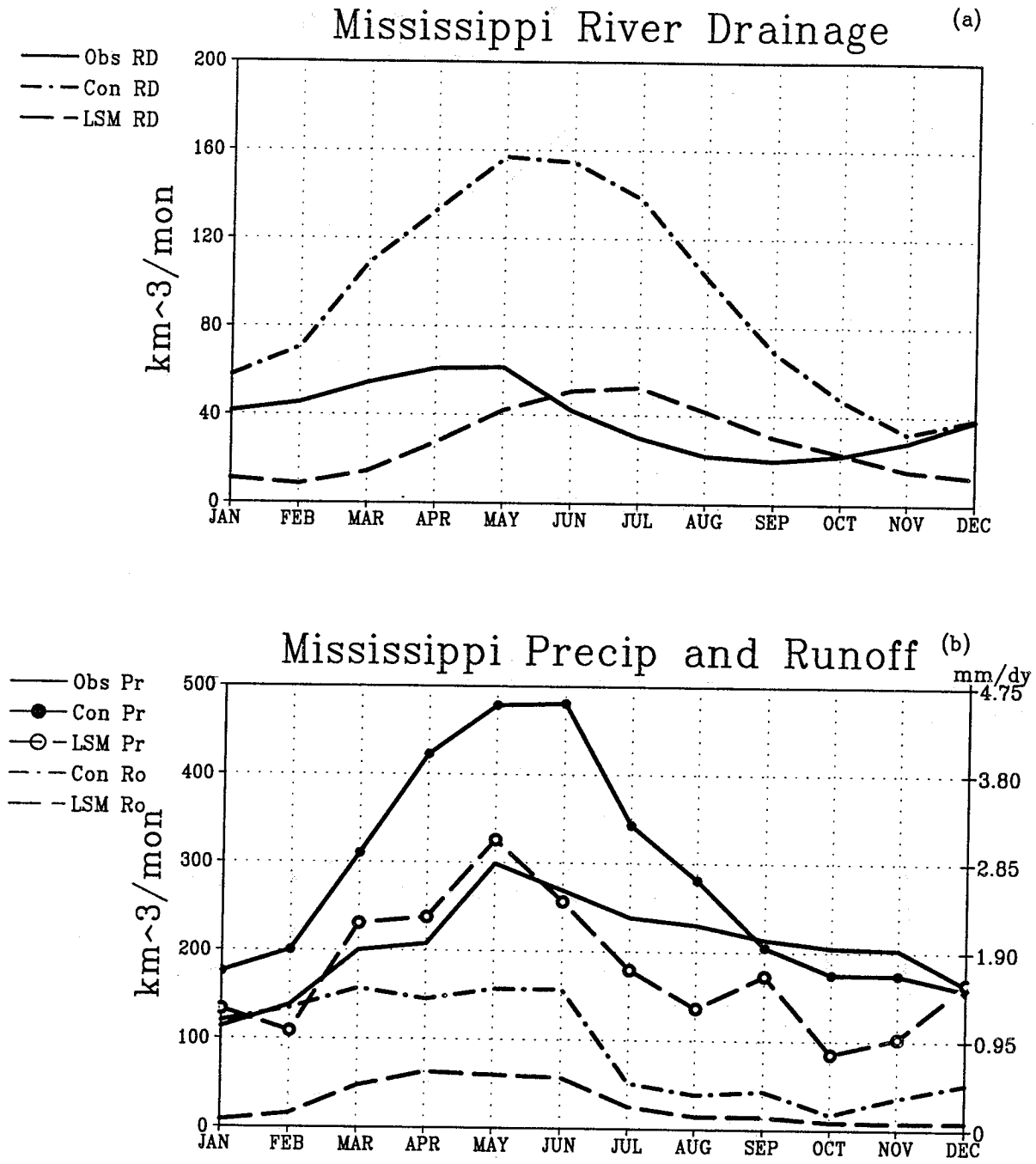

Figure 7. Annual cycle of (a) river discharge from the Mississippi River for observations, GCM-LSM and the GCM Control, and (b) precipitation and model source runoff.

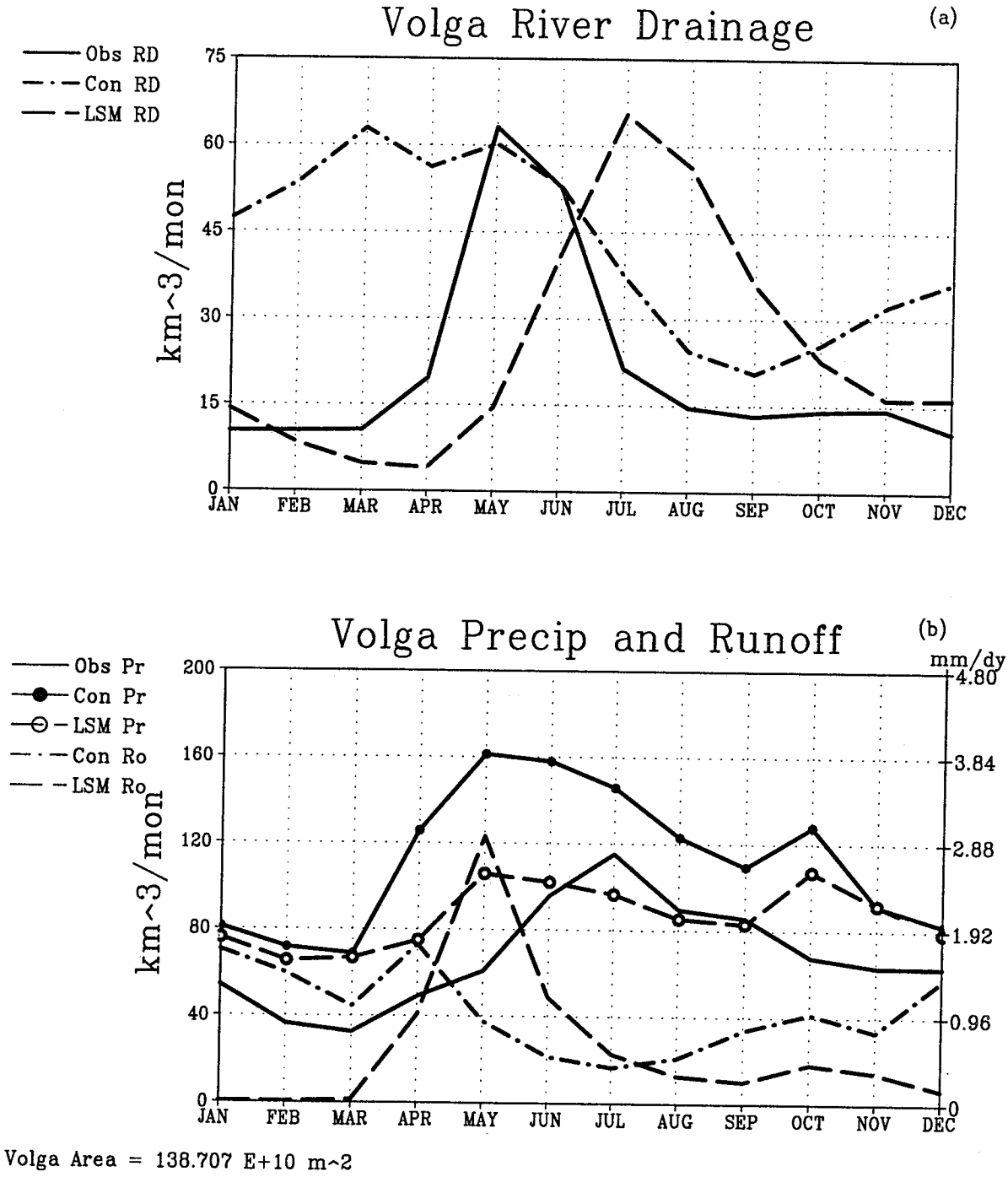

Figure 8. Annual cycle of (a) river discharge from the Volga River basin for observations, GCM-LSM and the GCM Control, and (b) precipitation and model source runoff.

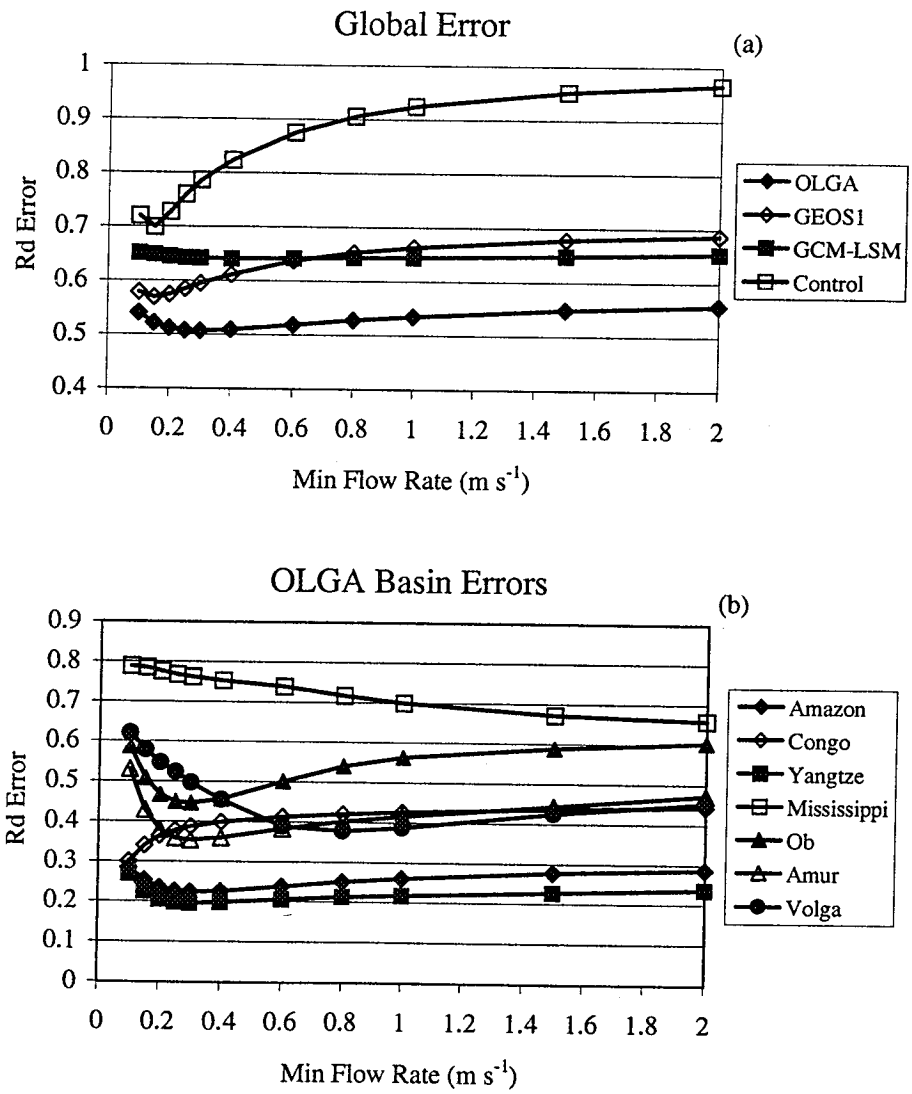

Figure 9. (a) Globally weighted river discharge error for different minimum flow rates. (b) OLGA river discharge error of various river basins for different minimum flow rates.